LA-UR-21-29181
Approved for public release; distribution is unlimited.

Title: Results from Computational study of TATB (LA-UR-21-20031)

Author(s): Wills, Ann Elisabet

Intended for: Report

Issued: 2021-09-16

Disclaimer:
Los Alamos National Laboratory, an affirmative action/equal opportunity employer, is operated by Triad National Security, LLC for the National Nuclear Security Administration of U.S. Department of Energy under contract 89233218CNA000001. By approving this article, the publisher recognizes that the U.S. Government retains nonexclusive, royalty-free license to publish or reproduce the published form of this contribution, or to allow others to do so, for U.S. Government purposes. Los Alamos National Laboratory requests that the publisher identify this article as work performed under the auspices of the U.S. Department of Energy. Los Alamos National Laboratory strongly supports academic freedom and a researcher's right to publish; as an institution, however, the Laboratory does not endorse the viewpoint of a publication or guarantee its technical correctness.

LANL REPORT

LA-UR-xx-xxxxx
Unlimited Release
Printed September 2021

Results from Computational study of TATB (LA-UR-21-20031)

Ann E. Mattsson

Published by
Los Alamos National Laboratory
Los Alamos, New Mexico 87545

Los Alamos National Laboratory, an affirmative action/equal opportunity employer, is managed by Triad National Security, LLC, for the National Nuclear Security Administration of the U.S. Department of Energy under contract 89233218CNA000001.

Approved for public release; further dissemination unlimited.

Produced at Los Alamos National Laboratory, operated for the United States Department of Energy by Triad National Security, LLC.

NOTICE: Los Alamos National Laboratory strongly supports academic freedom and a researcher's right to publish; as an institution, however, the Laboratory does not endorse the viewpoint of a publication or guarantee its technical correctness.

Printed in the United States of America.

Available to DOE and DOE contractors from
U.S. Department of Energy
Office of Scientific and Technical Information
P.O. Box 62
Oak Ridge, TN 37831

Telephone: (865) 576-8401
Facsimile: (865) 576-5728
E-Mail: reports@adonis.osti.gov
Online ordering: http://www.osti.gov/bridge

Available to the public from
U.S. Department of Commerce
National Technical Information Service
5285 Port Royal Rd
Springfield, VA 22161

Telephone: (800) 553-6847
Facsimile: (703) 605-6900
E-Mail: orders@ntis.fedworld.gov
Online ordering: http://www.ntis.gov/help/ordermethods.asp?loc=7-4-0#online

LA-UR-xx-xxxxx
Unlimited Release
Printed September 2021

Results from Computational study of TATB (LA-UR-21-20031)

Ann E. Mattsson
XCP-5 MS F644
Los Alamos National Laboratory
P.O. Box 1663, Los Alamos, NM 87545
aematts@lanl.gov

Abstract

This report is an addendum to "Computational study of TATB" (LA-UR-21-20031), explicitly giving results for future use and wrapping up some loose ends.

Acknowledgment

Los Alamos National Laboratory, an affirmative action/equal opportunity employer, is managed by Triad National Security, LLC, for the National Nuclear Security Administration of the U.S. Department of Energy under contract 89233218CNA000001.

Contents

Nomenclature **7**

1 Introduction and Summary **9**

Hugoniot points 9

Thermostat 11

2 Results: Static $T = 0\ K$. **13**

Structure at $T = 0$ Kelvin 13

3 Results: Hugoniot points. **17**

Two unit cells vertically (1x1x2) 17

Four unit cells in a plane (2x2x1) 19

Eight unit cells (2x2x2) 21

Determining Hugoniot points 23

Comparisons 30

References **31**

List of Figures

1.1 Pressure and temperature calculated with the AM05 functional using 3 different super cell sizes for each density: blue: 2 unit cells stacked vertically (1x1x2), red: 4 unit cells in a plane (2x2x1) and black: 8 unit cells (2x2x2). We expect the (black) points above 10 GPa to be accurate. 10

3.1 Determination of Hugoniot points from the jump conditions for density 2.25 g/cm^3, using 1x1x2 (top), 2x2x1 (middle), and 2x2x2 (bottom) super cells. . . 23

3.2 Determination of Hugoniot points from the jump conditions for density 2.48 g/cm^3, using 1x1x2 (top), 2x2x1 (middle), and 2x2x2 (bottom) super cells. . . 24

3.3 Determination of Hugoniot points from the jump conditions for density 2.74 g/cm^3, using 1x1x2 (top), 2x2x1 (middle), and 2x2x2 (bottom) super cells. . . 25

3.4 Determination of Hugoniot points from the jump conditions for density 3.03 g/cm^3, using 1x1x2 (top), 2x2x1 (middle), and 2x2x2 (bottom) super cells. . . 26

3.5 Determination of Hugoniot points from the jump conditions for density 3.37 g/cm^3, using 1x1x2 (top), 2x2x1 (middle), and 2x2x2 (bottom) super cells. . . 27

3.6 Determination of Hugoniot points from the jump conditions for density 3.77 g/cm^3, using 1x1x2 (top), 2x2x1 (middle), and 2x2x2 (bottom) super cells. The bottom plot shows two extra points (gray) for 8000 Kelvin where only the first half of the 20000+ MD steps are averaged over, giving accuracy of ordinary points calculated from 10000+ steps. Note the similar shift downwards for the energy and pressure based points. 28

3.7 Determination of Hugoniot points from the jump conditions for density 3.91 g/cm^3, using 1x1x2 (top), 2x2x1 (middle), and 2x2x2 (bottom) super cells. In the middle plot we used linear fit to three points to get our estimate and the origin is set at the 2 unit cell (top) Hugoniot point. Different fits yields values between this fit and the 12000 K point. 29

3.8 Our 8 unit cell Hugoniot data (red) compared to experimental data and fit from Ref. [20] (blue) and a theoretical PBX 9502 EOS derived in Ref. [4] (black). 30

Nomenclature

Hugoniot The collection of points in thermodynamic phase space describing the final states achievable by a shock from a specific initial state. The principal Hugoniot is the Hugoniot from the ambient state. Secondary Hugoniots can be obtained from pre-shocked states.

Quantum Mechanics The most fundamental and precise theory of matter that we know of. The theory of quantum particles, such as electrons and other elementary particles.

Quantum particle While the total energy of classical particles (composed of very many elementary particles) can be distributed continuously, the total energy of quantum particles is quantized. There are two types of quantum particles, fermions, such as electrons, and bosons, such as the Helium-4 atoms. While all bosons in a collection of bosons can have the same energy and form a Bose condensate, such as Helium-4 when it is superfluid, fermions in a collection of fermions, such as in a metal, need to all have different energies.

FD Fermi-Dirac statistics: The equilibrium distribution of energies in a collection of fermions at a certain temperature. This distribution is determining many of the properties of materials.

SE The Schrödinger Equation: The non-relativistic limit of the Dirac Equation, sufficiently accurate to describe electrons in lighter materials.

DFT Density Functional Theory: The formally exact reformulation of the wave-function based Shrödinger and Dirac Equations in terms of density and currents.[12]

KS The Kohn-Sham Equations: A calculational approach derived from the Dirac/SE using DFT. These are the equations implemented in DFT codes.[13]

Functional A short name for an approximation for the Exchange-Correlation functional which is the only part of DFT that needs to be approximated. The functional sets the possible accuracy of DFT calculations.

LMTO Linear Muffin Tin Orbital: A calculational method used in the RSPt code (see below).

LAPW Linear Augmented Plane Wave: Another calculational method. It is considered the implementation method that gives the most accurate DFT results. Other methods are usually verified against this method.

plane-wave code A code using plane waves as a basis set. This is the computationally most effective approach because Fourier Transforms can be used. Calculations can also be systematically improved by increasing the number of basis functions used, usually specified by the so called "cut-off". However, describing core electrons accurately requires a very large cut-off, leading to expensive calculations. The plane-wave approach thus is mostly used together with pseudo-potentials (see below).

all-electron code A code treating all electrons explicitly. LMTO and LAPW codes are all-electron.

pseudo-potential code The chemically inert core electrons are treated in a collective way via pseudo potentials, which increases the computational efficiency considerably. A number of different approaches exist; all are verified by comparing to all-electron, usually LAPW, results.

PAW Projected Augmented Wave: The pseudo potential technique currently considered the most accurate.[5,17]

VASP Vienna *Ab-initio* Simulation Package: A plane wave, pseudo potential (PAW), DFT code.[14–16]

core electron An electron close to the nucleus. In an LMTO or LAPW treatment these electrons are considered inert and their properties only depend on the closest nuclei. In a pseudo-potential code the effect of the core electrons on the valence electrons is included via pseudo potentials.

valence electron The outermost electrons are valence electrons and their properties are dependent on many nuclei. These electrons are forming bonds that hold a solid or molecule together.

Chapter 1

Introduction and Summary

This is an addendum to LA-UR-21-20031, "Calculational study of TATB" presenting all results in one compact publication.

Hugoniot points

We present results for 8 different volume principal Hugoniot points, including the standard temperature and pressure reference point. These points are calculated with the AM05 functional using the VASP code as described in Chapter 4 in LA-UR-21-20031, and using 3 different supercells, containing 96, 192, and 384 ions respectively. While AM05 cannot give good values for lower pressure due to its inability to handle the weak van der Waals' forces, we expect the 6 higher pressure points (> 10 GPa) to be accurate. In Fig. 1.1 we show that the temperature and pressure obtained for the three supercells at the same densities are differing minimally. Only the higher temperature points seems to differ and it is clear (see the Hugoniot determination plots at the end of this report) that the largest supercell gives the least scattering in data and thus gives the best fits. We should also note that 4 unit cells in a plane is not necessarily better than 2 unit cells stacked on top of each other. If the main result of a compression is that the planes pucker, the stacked unit cells supercell might be a better model of the system than the planar supercell.

We have performed a few non-standard calculations in order to make a preliminary verification of the here presented calculations. They are included in the tables, one longer than usual MD run in Table 3.5, and one (presumedly less accurate) calculation using velocity scaling instead of the Nosé thermostat in Table 3.1. None of these non-standard results deviate from our benchmark calculations in any significant way. In addition we note that the velocity scaling calculations used the same computational resources as the Nosé thermostat calculations, they were not faster.

Last we note that all the calculations we have made were started on the $T = 0$ K optimized structures. While the ion positions, of course, were allowed to change in the MD run, the symmetry of the supercell was not allowed to change. The influence of this constraint will be the topic of future studies.

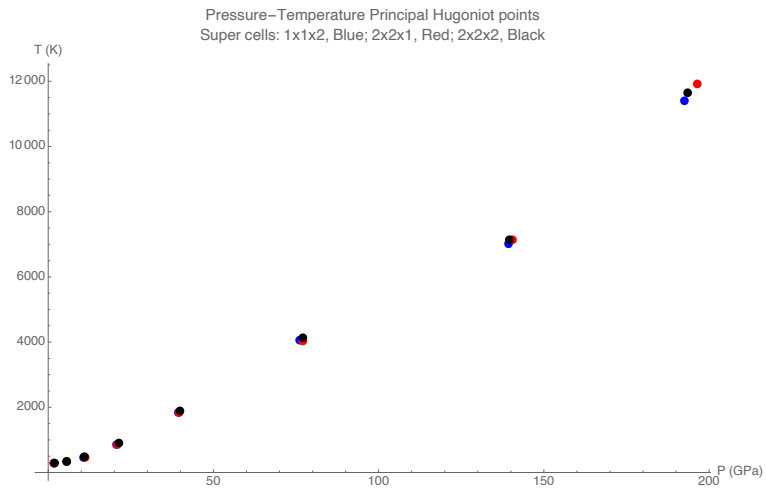

Figure 1.1: Pressure and temperature calculated with the AM05 functional using 3 different super cell sizes for each density: blue: 2 unit cells stacked vertically (1x1x2), red: 4 unit cells in a plane (2x2x1) and black: 8 unit cells (2x2x2). We expect the (black) points above 10 GPa to be accurate.

Thermostat

In publication LA-UR-21-20031, "Calculational study of TATB", Chapter 4, we discussed the value of SMASS and the periodicity of the temperature fluctuations. We ran a set of MD steps using SMASS = 37.24. The results showed a clear periodicity in all properties of a little less than 2000 time steps (of $0.2fs$), just as expected. However, since the oscillations were purely a result of the thermostat setting, there is no evidence that the system itself responded to these "natural" oscillations. We decided to not pursue this line of investigation further.

This page intentionally left blank.

Chapter 2

Results: Static $T = 0\ K$.

In this chapter we present results in table form corresponding to figures and discussions in Chapter 5 in LA-UR-21-20031.

Structure at $T = 0$ Kelvin

We here refer to the notation given in Figure 2.1. in LA-UR-21-20031.

Table 2.1: Structure and pressure (from VASP) for TATB according to LDA.

Density g/cm^3	Unitcell Volume Å^3	a Å	b Å	c Å	α °	β °	γ °	Pressure kB
3.63023	236.166	8.03230	8.04052	4.87731	115.083	91.1415	119.956	743.01
3.49903	245.021	8.09849	8.10842	4.96368	114.851	91.1720	119.952	617.07
3.37407	254.095	8.16285	8.17441	5.05173	114.597	91.2212	119.949	509.04
3.25500	263.390	8.22542	8.23848	5.14147	114.318	91.2882	119.945	416.64
3.14146	272.910	8.28617	8.30056	5.23302	114.020	91.3641	119.943	338.02
3.03315	282.655	8.34531	8.36082	5.32595	113.687	91.4683	119.942	271.31
2.92975	292.631	8.40252	8.41910	5.42063	113.331	91.5804	119.943	215.18
2.83101	302.838	8.45820	8.47574	5.51672	112.952	91.6999	119.945	167.93
2.73665	313.280	8.51210	8.53059	5.61484	112.563	91.8175	119.947	128.73
2.64644	323.959	8.56357	8.58276	5.71495	112.139	91.9395	119.952	96.43
2.56015	334.878	8.61434	8.63407	5.81568	111.700	92.0590	119.957	69.90
2.47757	346.039	8.66241	8.68224	5.91630	111.188	92.1696	119.965	48.45
2.39850	357.446	8.70927	8.72910	6.01691	110.648	92.2597	119.973	31.40
2.32277	369.101	8.75472	8.77424	6.11831	110.097	92.3068	119.981	17.86
2.25018	381.007	8.79614	8.81476	6.21197	109.351	92.2533	119.992	7.58
2.18060	393.166	8.83504	8.85264	6.29995	108.454	92.1186	120.004	-0.16
2.11385	405.581	8.87013	8.88635	6.36287	106.997	91.8266	120.018	-5.59
2.04980	418.254	8.90221	8.91756	6.41572	105.180	91.3297	120.029	-9.35
1.98831	431.189	8.93144	8.94545	6.52822	104.308	91.0701	120.035	-12.39
1.92925	444.388	8.96038	8.97408	6.66799	103.922	91.0194	120.040	-14.50
1.87251	457.853	8.98080	8.99430	6.80720	103.317	90.7206	120.036	-15.56

Table 2.2: Structure and pressure (from VASP) for TATB according to PBE.

Density g/cm^3	Unitcell Volume Å^3	a Å	b Å	c Å	α °	β °	γ °	Pressure kB
3.63023	236.166	8.03723	8.04799	4.87119	115.137	91.0864	119.957	896.66
3.49903	245.021	8.10427	8.11679	4.95709	114.921	91.1128	119.952	761.86
3.37407	254.095	8.16965	8.18380	5.04465	114.686	91.1543	119.947	645.26
3.25500	263.390	8.23345	8.24906	5.13391	114.435	91.2078	119.943	544.60
3.14146	272.910	8.29570	8.31258	5.22491	114.166	91.2785	119.938	457.95
3.03315	282.655	8.35643	8.37440	5.31767	113.880	91.3599	119.936	383.62
2.92975	292.631	8.41542	8.43430	5.41246	113.579	91.4499	119.935	319.97
2.83101	302.838	8.47324	8.49293	5.50879	113.265	91.5500	119.935	265.65
2.73665	313.280	8.52924	8.54958	5.60744	112.944	91.6465	119.937	219.61
2.64644	323.959	8.58408	8.60502	5.70754	112.597	91.7714	119.940	180.49
2.56015	334.878	8.63765	8.65907	5.80973	112.262	91.8687	119.944	147.54
2.47757	346.039	8.68891	8.71071	5.91502	111.934	91.9413	119.949	119.97
2.39850	357.446	8.73967	8.76155	6.02072	111.561	92.0601	119.956	96.89
2.32277	369.101	8.78875	8.81025	6.12877	111.185	92.1598	119.963	77.75
2.25018	381.007	8.83608	8.85740	6.23986	110.834	92.2209	119.971	61.87
2.18060	393.166	8.88313	8.90417	6.34742	110.410	92.2804	119.979	48.82
2.11385	405.581	8.92731	8.94811	6.45578	109.932	92.3210	119.988	38.10
2.04980	418.254	8.97015	8.99017	6.56927	109.515	92.3154	119.997	29.47
1.98831	431.189	9.01192	9.03049	6.67563	108.963	92.2566	120.008	22.52
1.92925	444.388	9.05122	9.06762	6.77030	108.170	92.1056	120.022	17.03
1.87251	457.853	9.08897	9.10577	6.90079	107.882	92.1114	120.024	12.36
1.81798	471.588	9.12642	9.14308	7.02955	107.496	92.1597	120.032	8.64
1.76554	485.594	9.16138	9.17758	7.16272	107.118	92.1746	120.039	5.74
1.71510	499.876	9.19156	9.20617	7.29283	106.499	92.1972	120.055	3.48
1.66656	514.434	9.22323	9.23731	7.43218	106.112	92.1838	120.060	1.71
1.61984	529.273	9.24526	9.25748	7.57051	105.385	92.1335	120.072	0.39
1.57484	544.394	9.26724	9.27823	7.70687	104.607	92.0393	120.082	-0.62
1.53150	559.801	9.29039	9.30061	7.86491	104.213	92.0062	120.087	-1.38
1.48974	575.495	9.30845	9.31754	8.02457	103.661	91.9334	120.090	-1.92
1.44948	591.480	9.32358	9.33166	8.19058	103.092	91.8479	120.093	-2.25
1.41065	607.758	9.33419	9.34151	8.36945	102.564	91.7693	120.095	-2.46
1.37320	624.333	9.34040	9.34691	8.55813	102.013	91.6838	120.095	-2.56

Table 2.3: Structure and pressure (from VASP) for TATB according to AM05.

Density g/cm^3	Unitcell Volume Å^3	a Å	b Å	c Å	α °	β °	γ °	Pressure kB
5.16882	165.867	7.36679	7.35475	4.16422	116.163	91.9137	119.954	3283.40
4.95930	172.874	7.44674	7.43886	4.23816	116.180	91.6635	119.967	2839.29

Table 2.3: Structure and pressure (from VASP) for TATB according to AM05.

Density g/cm^3	Unitcell Volume Å^3	a Å	b Å	c Å	α °	β °	γ °	Pressure kB
4.76095	180.077	7.52622	7.52058	4.31269	116.147	91.4792	119.971	2449.36
4.57304	187.476	7.60422	7.60091	4.38793	116.076	91.3365	119.971	2108.17
4.39489	195.076	7.68077	7.67956	4.46466	115.975	91.2353	119.971	1810.15
4.22588	202.878	7.75568	7.75673	4.54271	115.850	91.1616	119.969	1550.39
4.06542	210.885	7.82900	7.83214	4.62222	115.700	91.1165	119.967	1324.20
3.91298	219.100	7.90048	7.90568	4.70340	115.529	91.0913	119.963	1127.89
3.76807	227.526	7.97028	7.97743	4.78614	115.339	91.0844	119.959	957.71
3.63023	236.166	8.03830	8.04728	4.87058	115.130	91.0928	119.955	810.58
3.49903	245.021	8.10454	8.11532	4.95676	114.903	91.1163	119.951	683.67
3.37407	254.095	8.16901	8.18145	5.04468	114.657	91.1550	119.946	574.53
3.25500	263.390	8.23184	8.24577	5.13428	114.393	91.2063	119.942	480.89
3.14146	272.910	8.29289	8.30815	5.22572	114.109	91.2716	119.938	400.83
3.03315	282.655	8.35252	8.36888	5.31875	113.805	91.3513	119.936	332.64
2.92975	292.631	8.41037	8.42773	5.41369	113.484	91.4396	119.935	274.72
2.83101	302.838	8.46667	8.48487	5.51047	113.150	91.5294	119.936	225.81
2.73665	313.280	8.52155	8.54047	5.60894	112.801	91.6244	119.938	184.60
2.64644	323.959	8.57490	8.59440	5.70947	112.451	91.7084	119.941	150.08
2.56015	334.878	8.62677	8.64662	5.81181	112.086	91.7934	119.947	121.40
2.47757	346.039	8.67713	8.69713	5.91504	111.684	91.8915	119.952	97.65
2.39850	357.446	8.72577	8.74608	6.02170	111.315	91.9520	119.958	78.10
2.32277	369.101	8.77351	8.79341	6.12960	110.932	92.0026	119.964	62.10
2.25018	381.007	8.81915	8.83868	6.23758	110.511	92.0216	119.972	49.21
2.18060	393.166	8.86233	8.88202	6.34092	109.976	91.9922	119.982	38.63
2.11385	405.581	8.90555	8.92476	6.44830	109.477	91.9822	119.990	30.21
2.04980	418.254	8.94641	8.96397	6.54842	108.768	91.9472	120.005	23.55
1.98831	431.189	8.98482	9.00094	6.63805	107.803	91.8740	120.019	18.32
1.92925	444.388	9.01836	9.03219	6.64639	105.105	91.5203	120.046	14.78
1.87251	457.853	9.05510	9.06931	6.78110	104.865	91.5212	120.046	11.07
1.81798	471.588	9.09052	9.10470	6.91732	104.590	91.5012	120.050	8.26
1.76554	485.594	9.12140	9.13508	7.05749	104.226	91.4545	120.056	6.04
1.71510	499.876	9.15066	9.16393	7.20115	103.853	91.4053	120.062	4.33
1.66656	514.434	9.17987	9.19276	7.34630	103.481	91.3499	120.067	3.03
1.61984	529.273	9.19957	9.21141	7.49890	102.914	91.2177	120.075	2.00
1.57484	544.394	9.22089	9.23212	7.65783	102.480	91.1443	120.079	1.23
1.53150	559.801	9.24211	9.25280	7.82280	102.121	91.0964	120.083	0.64
1.48974	575.495	9.25731	9.26714	7.99429	101.640	90.9996	120.087	0.21
1.44948	591.480	9.27377	9.28292	8.17023	101.243	90.9359	120.089	-0.16
1.41065	607.758	9.29097	9.29968	8.35058	100.917	90.8952	120.092	-0.45
1.37320	624.333	9.30339	9.31132	8.53927	100.528	90.8350	120.092	-0.73
1.33707	641.206	9.31381	9.32109	8.73650	100.179	90.7919	120.094	-0.82

Table 2.3: Structure and pressure (from VASP) for TATB according to AM05.

Density	Unitcell Volume	a	b	c	α	β	γ	Pressure
g/cm^3	Å^3	Å	Å	Å	$\circ$	$\circ$	$\circ$	kB
1.30219	658.380	9.32521	9.33187	8.93509	99.8419	90.7481	120.093	-0.97
1.26851	675.858	9.33459	9.34073	9.14167	99.5302	90.7142	120.092	-1.06

Chapter 3

Results: Hugoniot points.

By performing 3-4 MD calculations per volume, at a few different temperatures, we were able to find the temperature, by interpolation, where the pressure and energy fulfills the jump conditions:

$$E_H - E_0 = -\frac{1}{2}(P_H + P_0)(V - V_0) \ . \tag{3.1}$$

I accordance with the discussion in Reference [23] we use the experimental equilibrium volume for V_0, set the temperature to 293 K, and obtain the values for E_0 and P_0 from an MD calculation. The reference point values are given first in each table. Note that E_0 is the internal energy and not the free energy. In the VASP OUTCAR file the internal energy is presented as '`energy without entropy`'.

For each super cell size we give the data evaluated from statistics (averaging) over the MD runs in table form. We present plots for the determination of the point where the Hugoniot jump conditions are valid and give the corresponding Hugoniot data in table form. For clarity we have gathered all plots for the same density together to allow for an easier comparison over super cells.

Two unit cells vertically (1x1x2)

Table 3.1: Calculated data for 2 unitcell TATB. The values in parenthesis is from a run using velocity scaling instead of the Nosé thermostat.

Density g/cm^3	Unitcell Volume Å^3	Temperature K	Pressure kB	Total Helmholtz free energy eV	Total Internal energy eV
1.92925	444.388	292.118	17.8091	-654.415	-654.413
2.25018	381.007	299.164	54.5478	-651.952	-651.952
2.25018	381.007	498.839	63.0623	-649.197	-649.183
2.25018	381.007	698.524	64.5815	-646.715	-646.707
2.47756	346.039	299.309	104.647	-648.749	-648.749
2.47756	346.039	498.709	108.768	-646.234	-646.234
2.47756	346.039	698.289	114.243	-643.701	-643.701

Table 3.1: Calculated data for 2 unitcell TATB. The values in parenthesis is from a run using velocity scaling instead of the Nosé thermostat.

Density g/cm^3	Unitcell Volume Å^3	Temperature K	Pressure kB	Total Helmholtz free energy eV	Total Internal energy eV
2.73664	313.280	698.257	203.755	-637.978	-637.978
2.73664	313.280	897.817	208.640	-635.413	-635.414
2.73664	313.280	1097.60	217.666	-632.794	-632.790
3.03315	282.655	1795.83	392.739	-613.541	-613.369
3.03315	282.655	1910.88	396.240	-611.769	-611.505
3.03315	282.655	1995.09	397.412	-610.723	-610.412
3.03315	282.655	2194.95	411.657	-603.431	-602.502
3.37408	254.095	3493.14	714.827	-577.448	-574.710
3.37408	254.095	4092.58	758.581	-566.333	-562.064
3.37408	254.095	4392.16	797.167	-558.145	-552.548
3.37408	254.095	4543.83	806.909	-553.150	-546.789
3.37408	254.095	4691.72	817.487	-552.043	-545.364
3.76809	227.525	5997.41	1307.29	-500.101	-487.320
3.76809	227.525	7196.88	1407.71	-480.396	-459.630
3.76809	227.525	7996.49	1462.35	-472.480	-445.786
3.91299	219.100	8996.66	1729.78	-449.959	-415.095
3.91299	219.100	9995.23	1813.33	-444.669	-400.909
3.91299	219.100	11195.3	1906.96	-440.907	-385.326
(3.91299	219.100	11200.0	1901.82	-440.785	-384.750)
3.91299	219.100	11994.6	1971.76	-437.033	-371.533

Table 3.2: Calculated Hugoniot points for 2 unit TATB.

Density g/cm^3	Unitcell Volume Å^3	Temperature K	Pressure kB	Total Internal energy eV
1.92925	444.388	292.118	17.8091	-654.413
2.25018	381.007	332.039	56.4307	-651.476
2.47756	346.039	462.209	107.913	-646.696
2.73664	313.280	852.372	207.165	-636.003
3.03315	282.655	1842.37	393.589	-612.884
3.37408	254.095	4054.03	760.183	-562.009
3.76809	227.525	7011.67	1393.65	-463.363
3.91299	219.100	11399.5	1924.49	-381.297

Four unit cells in a plane (2x2x1)

Table 3.3: Calculated data for 4 unitcell TATB.

Density g/cm^3	Unitcell Volume Å^3	Temperature K	Pressure kB	Total Helmholtz free energy eV	Total Internal energy eV
1.92925	444.388	292.188	17.6518	-1308.86	-1308.86
2.25018	381.008	299.152	54.7153	-1303.90	1303.90
2.25018	381.008	498.808	59.7734	-1298.90	-1298.90
2.25018	381.008	698.387	66.1822	-1293.84	-1293.84
2.47756	346.040	299.407	105.484	-1297.50	-1297.50
2.47756	346.040	498.808	111.328	-1292.47	-1292.47
2.47756	346.040	698.418	116.113	-1287.45	-1287.45
2.73664	313.280	698.266	204.287	-1276.02	-1276.02
2.73664	313.280	897.829	211.194	-1270.77	-1270.76
2.73664	313.280	1097.56	218.732	-1265.70	-1265.69
3.03315	282.655	1796.14	394.238	-1227.18	-1226.80
3.03315	282.655	1910.68	396.891	-1223.78	-1223.26
3.03315	282.655	1995.64	399.317	-1221.20	-1220.52
3.03315	282.655	2195.19	406.765	-1214.64	-1213.51
3.37408	254.095	3493.60	721.803	-1154.05	-1152.30
3.37408	254.095	4092.41	772.860	-1126.44	-1118.07
3.37408	254.095	4392.71	801.150	-1114.88	-1104.09
3.37408	254.095	4544.20	814.902	-1104.88	-1093.66
3.37408	254.095	4691.60	815.420	-1101.54	-1089.21
3.76805	227.528	5997.70	1308.24	-1003.16	-978.011
3.76805	227.528	7197.75	1407.96	-963.106	-921.910
3.76805	227.528	7997.71	1470.57	-942.744	-889.202
3.91299	219.100	8996.85	1727.17	-908.695	-840.683
3.91299	219.100	9996.15	1810.46	-888.999	-801.922
3.91299	219.100	11196.6	1903.58	-882.599	-770.734
3.91299	219.100	11994.7	1970.90	-878.084	-749.631

Table 3.4: Calculated Hugoniot points for 4 unit TATB.

Density g/cm^3	Unitcell Volume Å^3	Temperature K	Pressure kB	Total Internal energy eV
1.92925	444.388	292.188	17.6518	-1308.86
2.25018	381.008	332.243	56.4600	-1303.08
2.47756	346.040	473.418	110.643	-1293.11
2.73664	313.280	865.604	210.036	-1271.60
3.03315	282.655	1838.36	395.123	-1225.52
3.37408	254.095	4033.41	771.415	-1121.42
3.76805	227.528	7150.22	1404.14	-923.972
3.91299	219.100	$\sim$ 11920	$\sim$ 1964	$\sim$ -752

Eight unit cells (2x2x2)

Table 3.5: Calculated data for 8 unitcell TATB. The values in parenthesis are calculated from averaging over only half of the 20000+ MD steps in the special run above them in the table, giving approximate error bars due to finite sampling in our ordinary runs which uses 10000+ MD steps.

Density g/cm^3	Unitcell Volume Å^3	Temperature K	Pressure kB	Total Helmholtz free energy eV	Total Internal energy eV
1.92925	444.388	292.388	19.4122	-2617.78	-2617.78
2.25018	381.008	299.254	55.8304	-2607.84	-2607.84
2.25018	381.008	343.112	55.8349	-2605.63	-2605.63
2.25018	381.008	498.810	60.1126	-2597.85	-2597.85
2.25018	381.008	698.456	65.6188	-2587.68	-2587.68
2.47757	346.039	299.322	105.937	-2595.04	-2595.04
2.47757	346.039	498.854	110.420	-2585.00	-2585.00
2.47757	346.039	698.350	116.469	-2574.85	-2574.85
2.73664	313.280	698.588	207.165	-2551.92	-2551.91
2.73664	313.280	898.021	212.886	-2541.77	-2541.77
2.73664	313.280	1097.51	218.379	-2531.31	-2531.30
3.03315	282.655	1795.85	397.652	-2454.20	-2453.46
3.03315	282.655	1910.85	400.179	-2447.91	-2446.87
3.03315	282.655	1995.52	403.087	-2442.74	-2441.43
3.03315	282.655	2195.18	408.343	-2427.91	-2425.57
3.37408	254.095	3493.32	705.905	-2315.15	-2304.15
3.37408	254.095	4092.75	770.560	-2264.80	-2247.34
3.37408	254.095	4392.45	795.514	-2236.20	-2214.24
3.37408	254.095	4543.69	796.064	-2219.30	-2194.49
3.37408	254.095	4691.65	817.646	-2212.51	-2185.87
3.76807	227.526	5997.96	1312.21	-2000.33	-1949.28
3.76807	227.526	7196.88	1399.96	-1929.30	-1846.64
3.76807	227.526	7996.85	1470.03	-1889.35	-1782.54
(3.76807	227.526	7996.86	1466.83	-1890.88	-1783.99)
3.91299	219.100	8996.92	1733.81	-1808.51	-1671.30
3.91299	219.100	9995.35	1811.87	-1782.43	-1608.09
3.91299	219.100	11195.8	1900.63	-1768.40	-1545.15
3.91299	219.100	11995.7	1960.44	-1759.06	-1499.60

Table 3.6: Calculated Hugoniot points for 8 unit TATB.

Density g/cm^3	Unitcell Volume Å^3	Temperature K	Pressure kB	Total Internal energy eV
1.92925	444.388	292.388	19.4122	-2617.78
2.25018	381.008	339.993	56.2779	-2605.80
2.47757	346.039	478.455	109.890	-2586.03
2.73664	313.280	898.645	212.904	-2541.74
3.03315	282.655	1885.42	399.861	-2448.49
3.37408	254.095	4126.38	771.778	-2241.90
3.76807	227.526	7127.49	1394.32	-1852.37
3.91299	219.100	11646.8	1934.65	-1518.71

Determining Hugoniot points

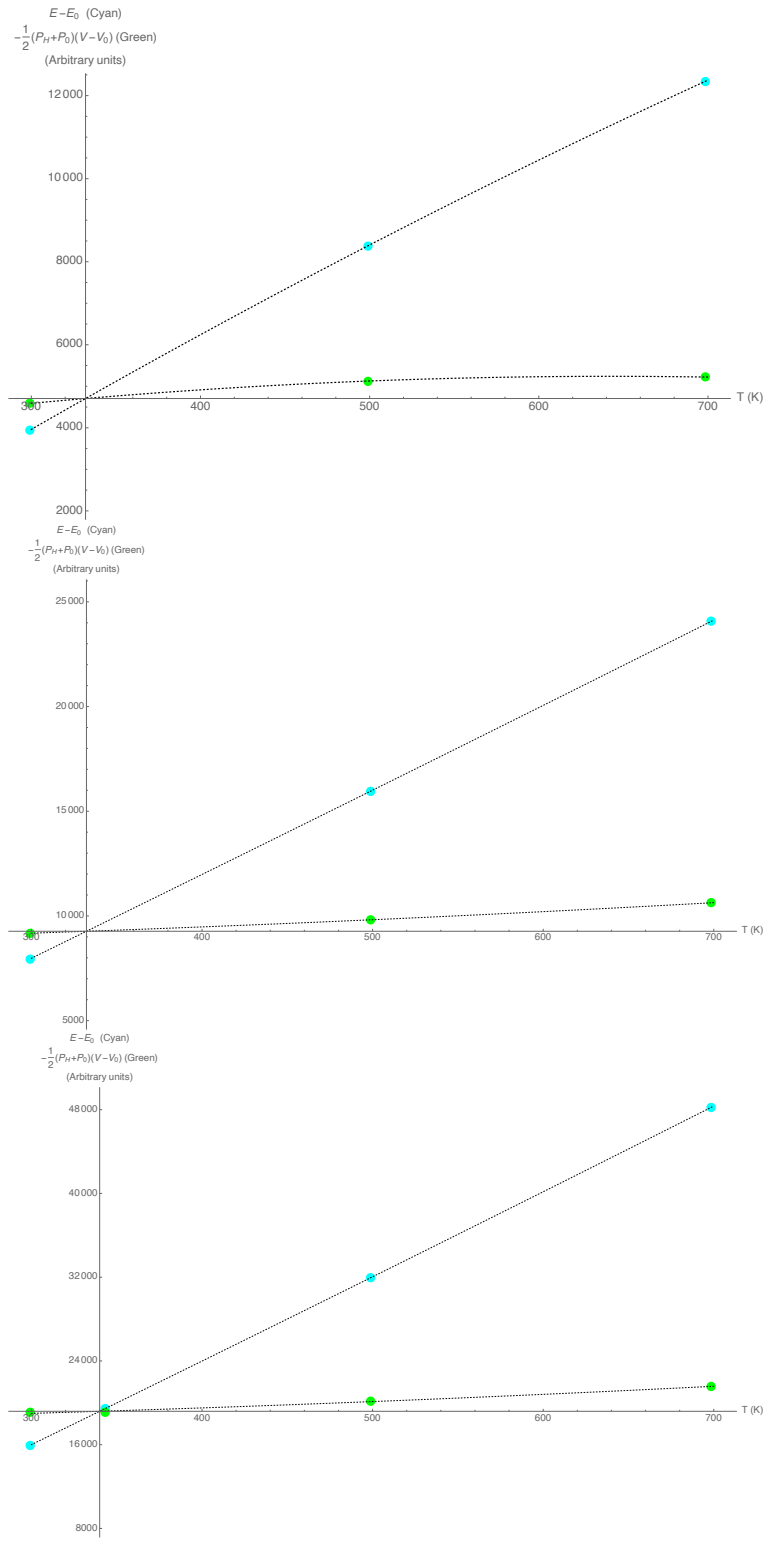

Figure 3.1: Determination of Hugoniot points from the jump conditions for density 2.25 g/cm^3, using 1x1x2 (top), 2x2x1 (middle), and 2x2x2 (bottom) super cells.

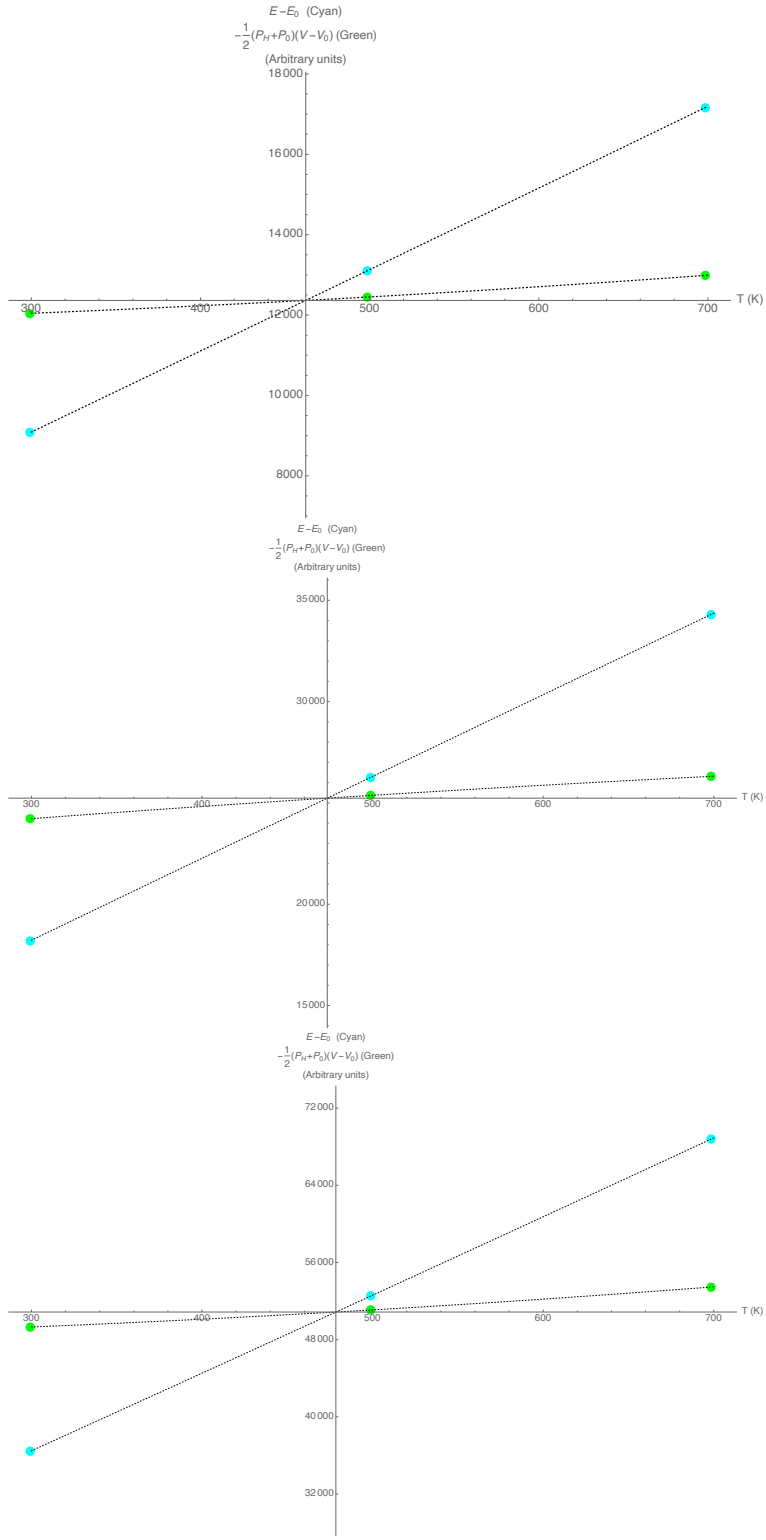

Figure 3.2: Determination of Hugoniot points from the jump conditions for density 2.48 g/cm^3, using 1x1x2 (top), 2x2x1 (middle), and 2x2x2 (bottom) super cells.

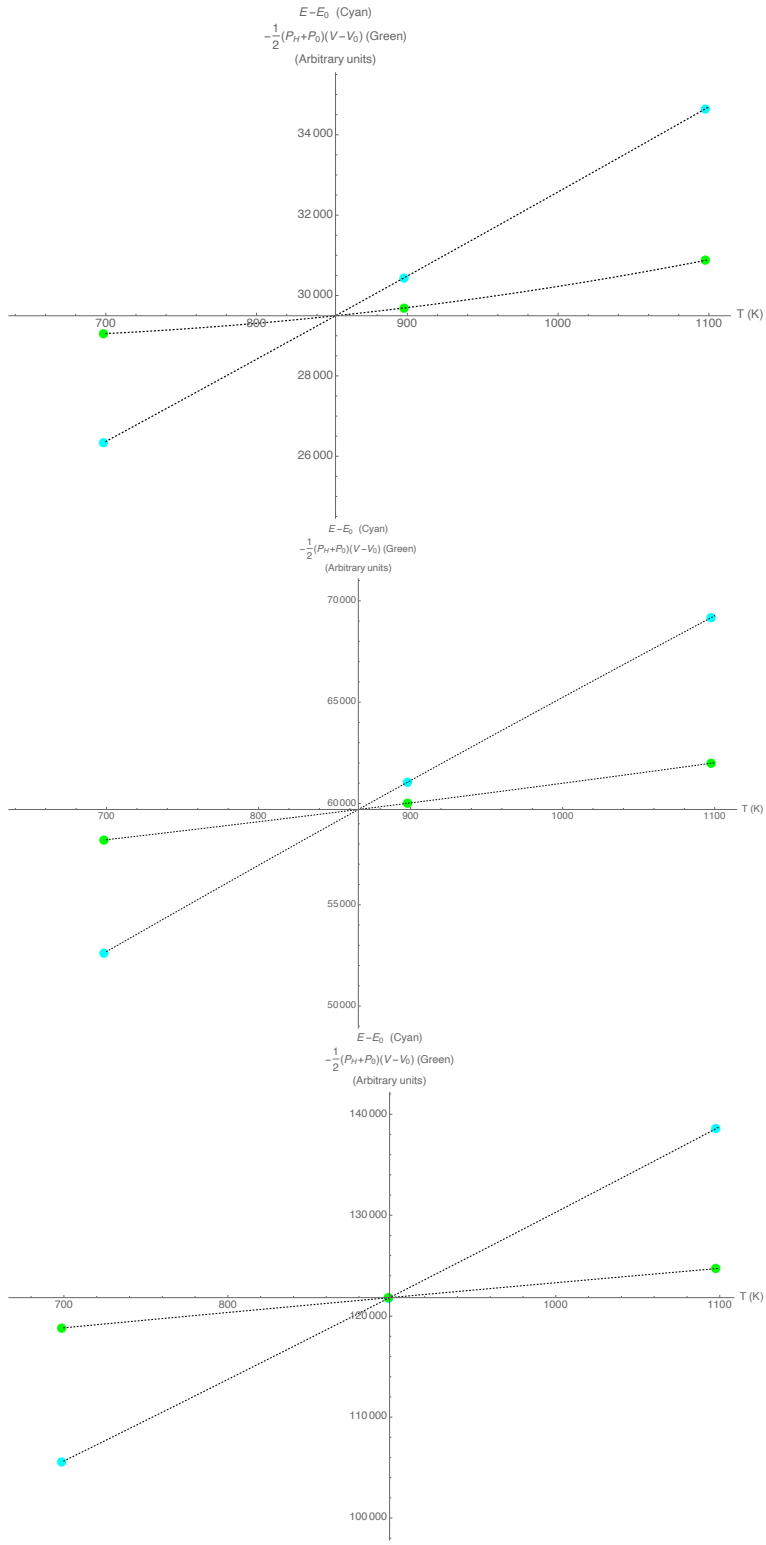

Figure 3.3: Determination of Hugoniot points from the jump conditions for density 2.74 g/cm^3, using 1x1x2 (top), 2x2x1 (middle), and 2x2x2 (bottom) super cells.

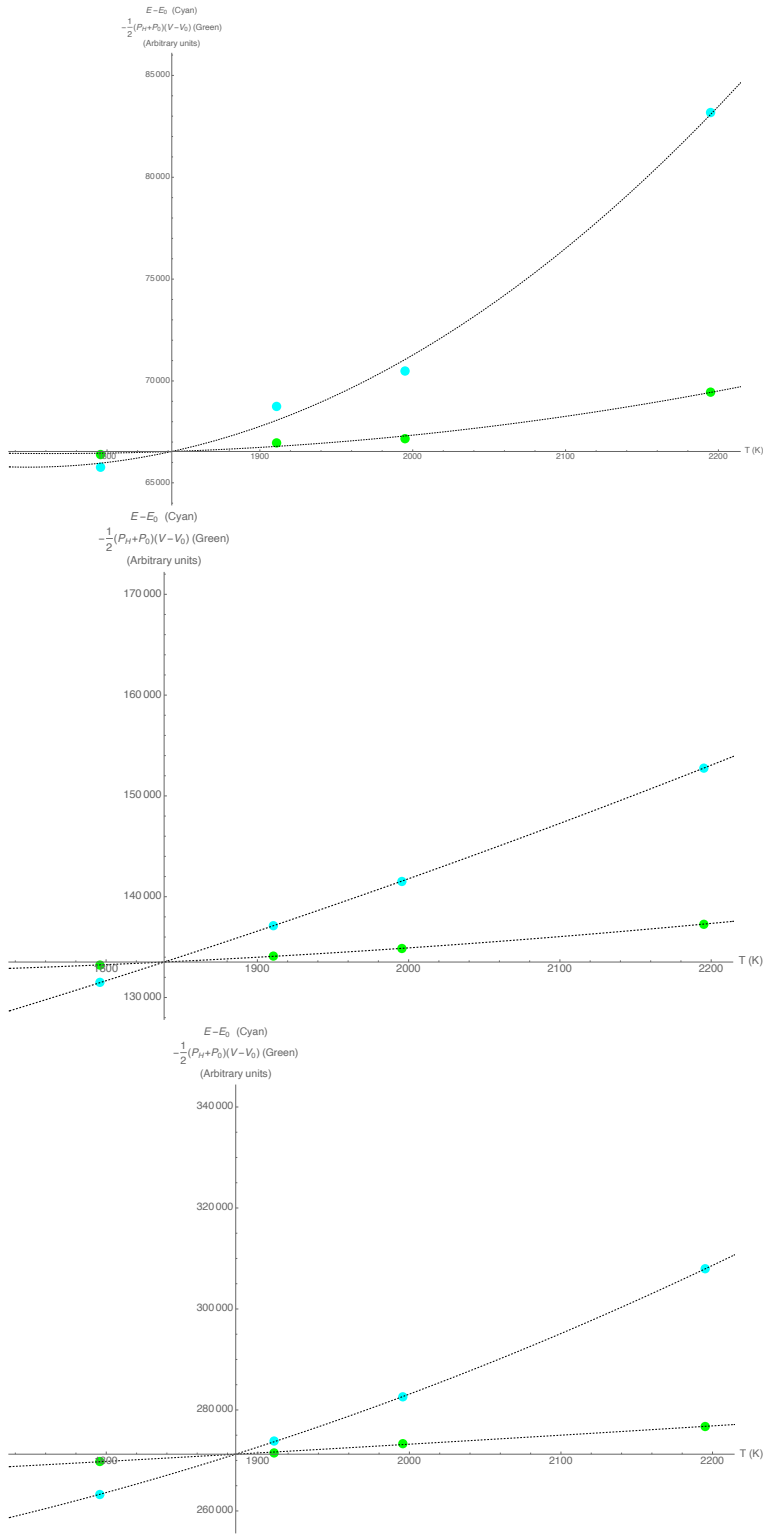

Figure 3.4: Determination of Hugoniot points from the jump conditions for density 3.03 g/cm^3, using 1x1x2 (top), 2x2x1 (middle), and 2x2x2 (bottom) super cells.

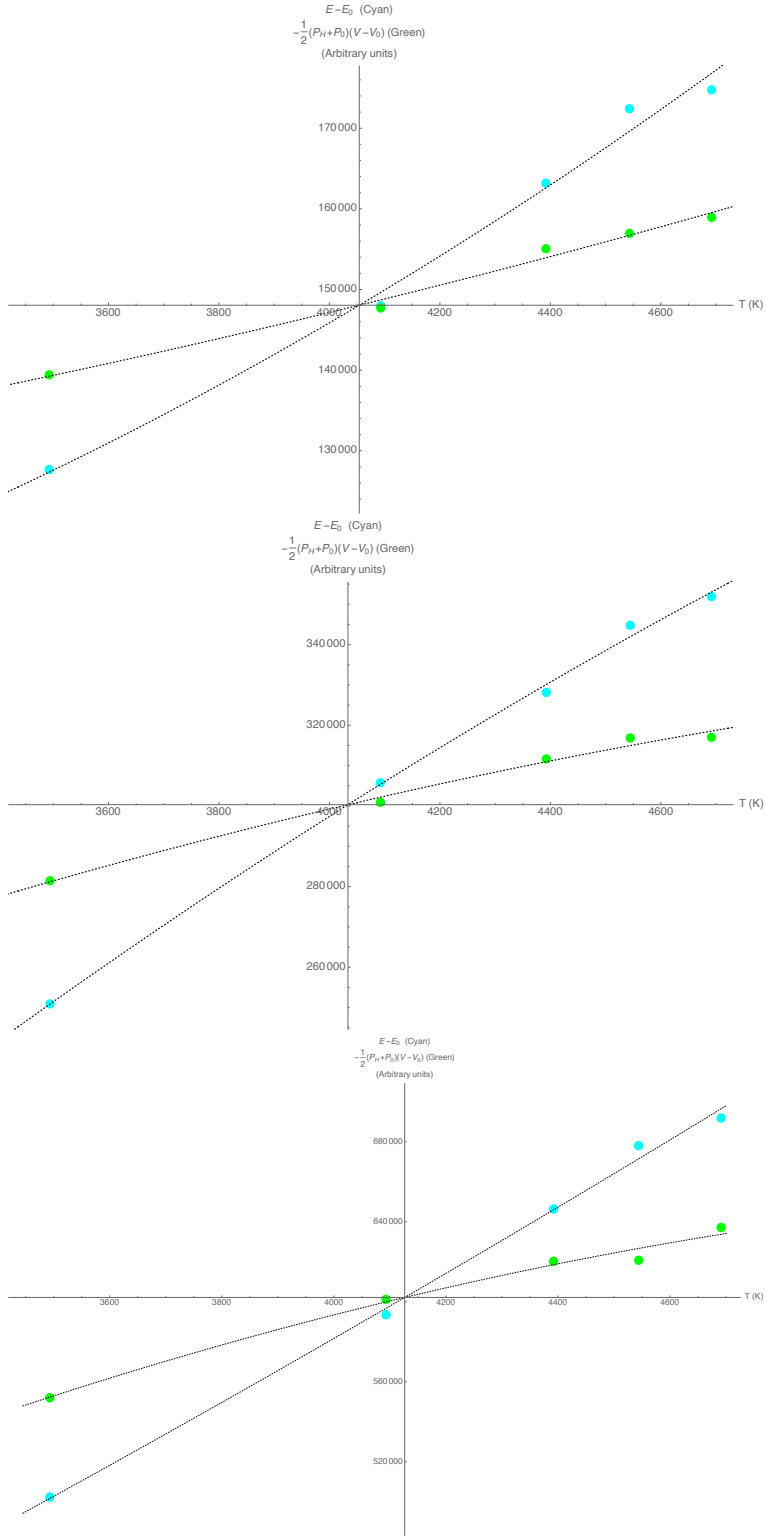

Figure 3.5: Determination of Hugoniot points from the jump conditions for density 3.37 g/cm^3, using 1x1x2 (top), 2x2x1 (middle), and 2x2x2 (bottom) super cells.

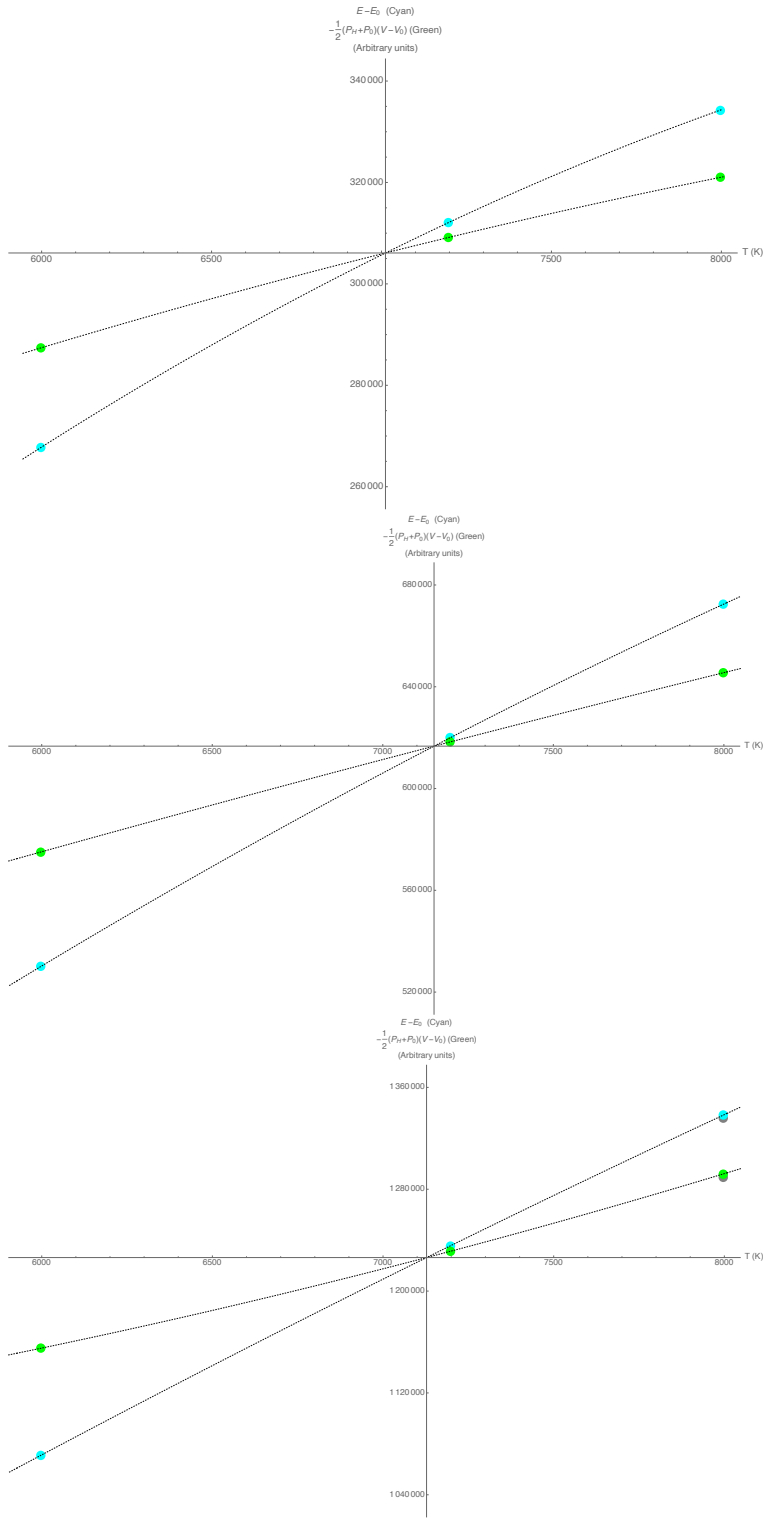

Figure 3.6: Determination of Hugoniot points from the jump conditions for density 3.77 g/cm^3, using 1x1x2 (top), 2x2x1 (middle), and 2x2x2 (bottom) super cells. The bottom plot shows two extra points (gray) for 8000 Kelvin where only the first half of the 20000+ MD steps are averaged over, giving accuracy of ordinary points calculated from 10000+ steps. Note the similar shift downwards for the energy and pressure based points.

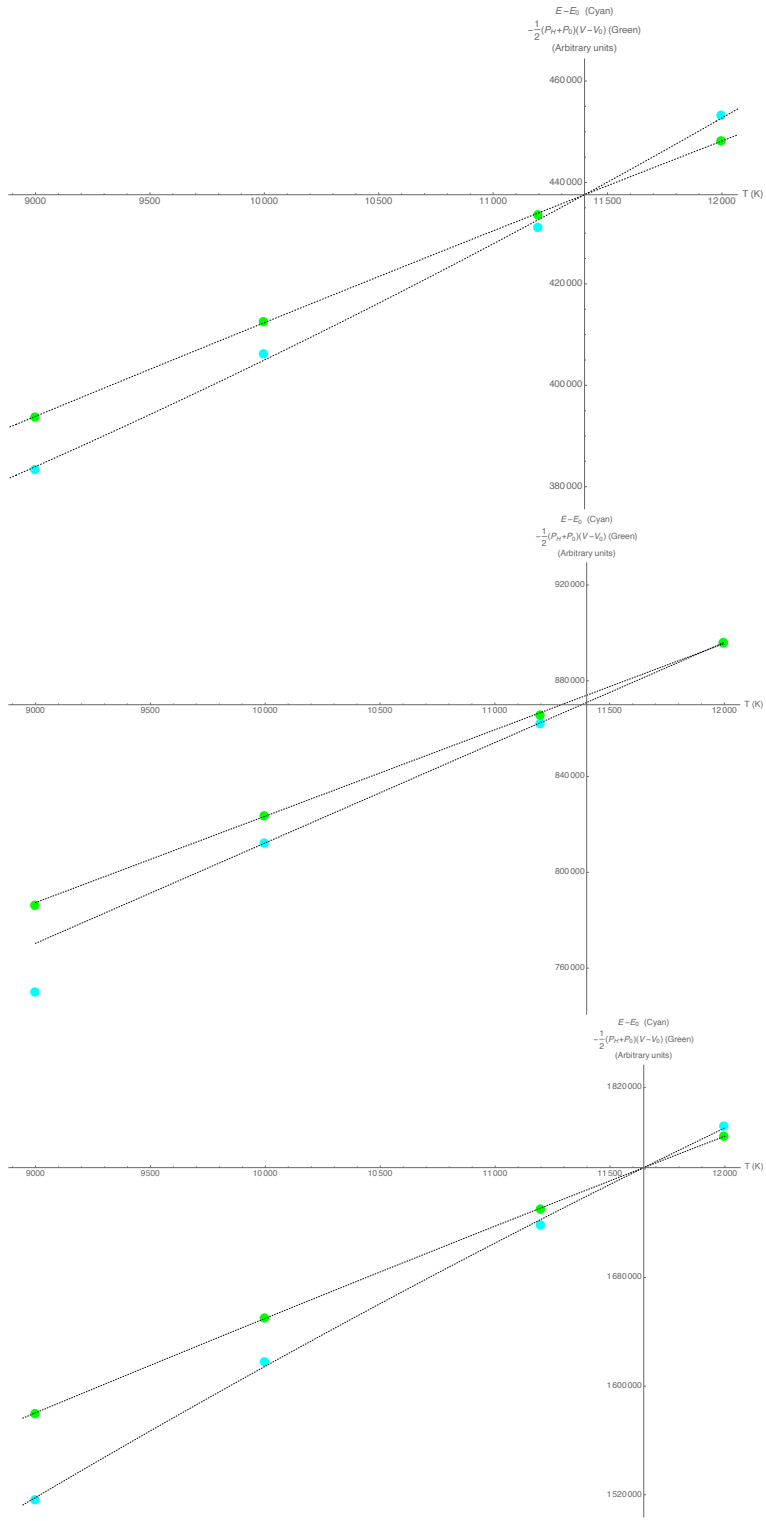

Figure 3.7: Determination of Hugoniot points from the jump conditions for density 3.91 g/cm^3, using 1x1x2 (top), 2x2x1 (middle), and 2x2x2 (bottom) super cells. In the middle plot we used linear fit to three points to get our estimate and the origin is set at the 2 unit cell (top) Hugoniot point. Different fits yields values between this fit and the 12000 K point.

Comparisons

Finally we compare our 8 unit cells calculations with other published results. Figure 3.8 shows the final data and replaces Fig. 6.2. and 6.3. in LA-UR-21-20031. Our data shows a stiffer Hugoniot than what is given by the Aslam EOS and the extrapolated fit to the recent experimental data from Ref. 20. However, in the interpolating region of the fit the 3 different Hugoniot curves represents the experimental data equally well. We should note that one benefit from using DFT for calculating Hugoniot curves is that we get temperatures. Interestingly, in our case the temperatures obtained with VASP do NOT correspond well to the temperatures these points would give using the Aslam EOS. How this would influence real hydro code results cannot be assessed until a new EOS based on our data have been constructed, and is left for future projects.

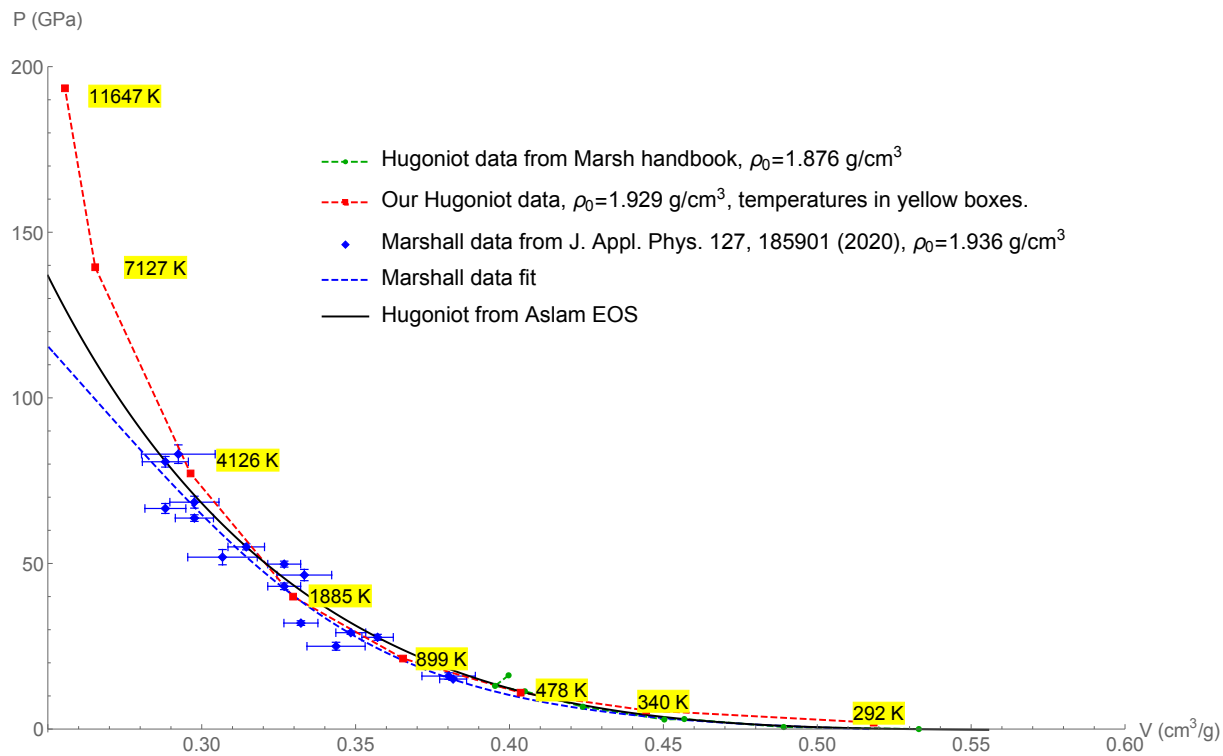

Figure 3.8: Our 8 unit cell Hugoniot data (red) compared to experimental data and fit from Ref. [20] (blue) and a theoretical PBX 9502 EOS derived in Ref. [4] (black).

References

[1] From https://chemapps.stolaf.edu/jmol/jmol.php via Wikipedia, https://www.wikipedia.org. Jmol: an open-source Java viewer for chemical structures in 3D. http://www.jmol.org/.

[2] R. Armiento and A. Mattsson. Alternative separation of exchange and correlation in density-functional theory. *Phys. Rev. B*, 68:245120, Dec 2003.

[3] R. Armiento and A. E. Mattsson. Functional designed to include surface effects in self-consistent density functional theory. *Phys. Rev. B*, 72:085108, Aug 2005.

[4] Tariq D. Aslam. The reactants equation of state for the tri-amino-tri-nitro-benzene (TATB) based explosive PBX 9502. *Journal of Applied Physics*, 122(3):035902, 2017.

[5] P. E. Blöchl. Projector augmented-wave method. *Phys. Rev. B*, 50:17953–17979, Dec 1994.

[6] Peter E. Blöchl, O. Jepsen, and O. K. Andersen. Improved tetrahedron method for brillouin-zone integrations. *Phys. Rev. B*, 49:16223–16233, Jun 1994.

[7] H. H. Cady and A. C. Larson. The crystal structure of 1,3,5-triamino-2,4,6-trinitrobenzene. *Acta Crystallographica*, 18(3):485–496, Mar 1965.

[8] D. M. Ceperley and B. J. Alder. Ground state of the electron gas by a stochastic method. *Phys. Rev. Lett.*, 45:566–569, Aug 1980.

[9] Alistair J. Davidson, Ranga P. Dias, Dana M. Dattelbaum, and Choong-Shik Yoo. "Stubborn" triaminotrinitrobenzene: Unusually high chemical stability of a molecular solid to 150 GPa. *The Journal of Chemical Physics*, 135(17):174507, 2011.

[10] Stefan Grimme. Semiempirical GGA-type density functional constructed with a long-range dispersion correction. *Journal of Computational Chemistry*, 27(15):1787–1799, 2006.

[11] Philipp Haas, Fabien Tran, and Peter Blaha. Calculation of the lattice constant of solids with semilocal functionals. *Phys. Rev. B*, 79:085104, Feb 2009.

[12] P. Hohenberg and W. Kohn. Inhomogeneous electron gas. *Phys. Rev.*, 136:B864–B871, Nov 1964.

[13] W. Kohn and L. J. Sham. Self-consistent equations including exchange and correlation effects. *Phys. Rev.*, 140:A1133–A1138, Nov 1965.

[14] G. Kresse and J. Furthmüller. Efficient iterative schemes for *ab initio* total-energy calculations using a plane-wave basis set. *Phys. Rev. B*, 54:11169–11186, Oct 1996.

[15] G. Kresse and J. Hafner. Ab initio molecular dynamics for liquid metals. *Phys. Rev. B*, 47:R558, 1993.

[16] G. Kresse and J. Hafner. Ab initio molecular-dynamics simulation of the liquid-metal-amorphous-semiconductor transition in germanium. *Phys. Rev. B*, 49:14251, 1994.

[17] G. Kresse and D. Joubert. From ultrasoft pseudopotentials to the projector augmented-wave method. *Phys. Rev. B*, 59:1758–1775, Jan 1999.

[18] Kurt Lejaeghere, Gustav Bihlmayer, Torbjörn Björkman, Peter Blaha, Stefan Blügel, Volker Blum, Damien Caliste, Ivano E. Castelli, Stewart J. Clark, Andrea Dal Corso, Stefano de Gironcoli, Thierry Deutsch, John Kay Dewhurst, Igor Di Marco, Claudia Draxl, Marcin Dułak, Olle Eriksson, José A. Flores-Livas, Kevin F. Garrity, Luigi Genovese, Paolo Giannozzi, Matteo Giantomassi, Stefan Goedecker, Xavier Gonze, Oscar Grånäs, E. K. U. Gross, Andris Gulans, François Gygi, D. R. Hamann, Phil J. Hasnip, N. A. W. Holzwarth, Diana Iuşan, Dominik B. Jochym, François Jollet, Daniel Jones, Georg Kresse, Klaus Koepernik, Emine Küçükbenli, Yaroslav O. Kvashnin, Inka L. M. Locht, Sven Lubeck, Martijn Marsman, Nicola Marzari, Ulrike Nitzsche, Lars Nordström, Taisuke Ozaki, Lorenzo Paulatto, Chris J. Pickard, Ward Poelmans, Matt I. J. Probert, Keith Refson, Manuel Richter, Gian-Marco Rignanese, Santanu Saha, Matthias Scheffler, Martin Schlipf, Karlheinz Schwarz, Sangeeta Sharma, Francesca Tavazza, Patrik Thunström, Alexandre Tkatchenko, Marc Torrent, David Vanderbilt, Michiel J. van Setten, Veronique Van Speybroeck, John M. Wills, Jonathan R. Yates, Guo-Xu Zhang, and Stefaan Cottenier. Reproducibility in density functional theory calculations of solids. *Science*, 351(6280), 2016.

[19] S. P. Marsh. *LASL shock Hugoniot data*. University of California Press, Berkeley a.o, 1980.

[20] M. C. Marshall, A. Fernandez-Pañella, T. W. Myers, J. H. Eggert, D. J. Erskine, S. Bastea, L. E. Fried, and L. D. Leininger. Shock hugoniot measurements of single-crystal 1,3,5-triamino-2,4,6-trinitrobenzene (TATB) compressed to 83 GPa. *Journal of Applied Physics*, 127(18):185901, 2020.

[21] Ann E. Mattsson. In pursuit of the "divine" functional. *Science*, 298(5594):759–760, 2002.

[22] Ann E. Mattsson. A lithium projector augmented wave potential suitable for use in vasp at high compression and temperature. Technical report SAND2012-7389, Sandia National Laboratories, Albuquerque, New Mexico 87185 and Livermore, California 94550, September 2012.

[23] Ann E. Mattsson, Ryan R. Wixom, and Thomas R. Mattsson. Calculating hugoniots for molecular crystals from first principles. In *Proceedings of 14th International Detonation Symposium, April 11-16, 2010*, page 1043. ONR-351-10-185, 2010.

[24] Shawn D. McGrane, Tariq D. Aslam, Timothy H. Pierce, Steven J. Hare, and Mark E. Byers. Temperature of shocked plastic bonded explosive PBX 9502 measured with spontaneous Stokes/anti-Stokes Raman. *Journal of Applied Physics*, 123(4):045902, 2018.

[25] Hendrik J. Monkhorst and James D. Pack. Special points for brillouin-zone integrations. *Phys. Rev. B*, 13:5188–5192, Jun 1976.

[26] Shuichi Nosé. A unified formulation of the constant temperature molecular dynamics methods. *The Journal of Chemical Physics*, 81(1):511–519, 1984.

[27] J. P. Perdew and Alex Zunger. Self-interaction correction to density-functional approximations for many-electron systems. *Phys. Rev. B*, 23:5048–5079, May 1981.

[28] John Perdew and Yue Wang. Accurate and simple analytic representation of the electron-gas correlation energy. *Phys. Rev. B*, 45:13244–13249, Jun 1992.

[29] John P. Perdew, Kieron Burke, and Matthias Ernzerhof. Generalized gradient approximation made simple. *Phys. Rev. Lett.*, 77:3865–3868, Oct 1996.

[30] Thomas Plisson, Nicolas Pineau, Gunnar Weck, Eric Bruneton, Nicolas Guignot, and Paul Loubeyre. Equation of state of 1,3,5-triamino-2,4,6-trinitrobenzene up to 66 GPa. *Journal of Applied Physics*, 122(23):235901, 2017.

[31] The RSPt code. See http://fplmto-rspt.org/.

[32] S. H. Vosko, L. Wilk, and M. Nusair. Accurate spin-dependent electron liquid correlation energies for local spin density calculations: a critical analysis. *Canadian Journal of Physics*, 58(8):1200–1211, 1980.

[33] J. M. Wills, O. Eriksson, M. Alouani, and D. L. Price. Full potential LMTO: Total energy and force calculations. In H. Dreysse, editor, *Electronic Structure and Physical Properties of Solids: The Uses of the LMTO Method*, volume 535 of *Lecture Notes in Physics*. Springer-Verlag, Berlin, 2000.

This page intentionally left blank.

Los Alamos National Laboratory, an affirmative action/equal opportunity employer, is managed by Triad National Security, LLC, for the National Nuclear Security Administration of the U.S. Department of Energy under contract 89233218CNA000001.